Efficient Light-Harvesting Systems with Tunable Emission through Controlled Precipitation in Confined Nanospace

Chuanqi Li, Jing Zhang, Shiyong Zhang, and Yan Zhao*

Abstract: *Light harvesting is a key step in photosynthesis but creation of synthetic light-harvesting systems (LHSs) with high efficiencies has been challenging. When donor and acceptor dyes with aggregation-induced emission were trapped within the interior of cross-linked reverse vesicles, LHSs were obtained readily through spontaneous hydrophobically driven aggregation of the dyes in water. Aggregation in the confined nanospace was critical to the energy transfer and the light-harvesting efficiency. The efficiency of the excitation energy transfer (EET) reached 95 % at a donor/acceptor ratio of 100:1 and the energy transfer was clearly visible even at a donor/acceptor ratio of 10 000:1. Multicolor emission was achieved simply by tuning the donor/acceptor feed ratio in the preparation and the quantum yield of white light emission from the system was 0.38, the highest reported for organic materials in water to date.*

The natural photosynthetic unit (PSU) is a highly efficient Einstein photochemical machine for converting light energy into chemical potential.[1] In higher plants and green algae, the unit comprises two photosystems, I and II, that each employ 200–400 antenna chromophores to harvest photons under ambient light. Over the last decades, the importance of the process has motivated generations of researchers to perform structural characterization, to study the intricacies of the mechanisms, and to mimic key steps of the process for potential applications in photosynthesis, photocatalysis, and photovoltaics.[2]

To mimic the natural light-harvesting systems (LHSs), chemists have used many scaffolds including dendrimers,[3] organogels,[4] micelles,[5] vesicles,[6] host-guest assemblies,[7] organic nanocrystals,[8] metal–organic frameworks,[9] polymer nanoparticles,[10] biomacromolecule assemblies,[11] and others.[12] Impressive progress has been made in recent years, particularly in the spatial organization of multichromophores to enhance the efficiency of excitation energy transfer (EET) and minimize self-quenching.

[*] C. Li, J. Zhang, Prof. S. Zhang
National Engineering Research Center for Biomaterials, and College of Chemistry, Sichuan University
29 Wangjiang Road, Chengdu 610064 (China)
E-mail: szhang@scu.edu.cn
Prof. Y. Zhao
Department of Chemistry, Iowa State University
Ames, IA 50011-3111 (USA)

The LHSs reported so far can be broadly classified into two groups, those constructed on a covalent framework and those obtained through self-assembly. The former has the benefit of high stability but often requires substantial synthetic efforts. The latter can be conveniently obtained by mixing appropriate ingredients under suitable conditions but tend to be unstable. The natural PSU, on the other hand, is a membrane-based system compartmentalized with specialized components. A combination of covalent and noncovalent strategies is utilized for the construction of the final hierarchical structure. The membrane-enclosed architecture is crucial to photosynthesis, as production, transport, and accumulation of protons on the membrane creates proton motive forces needed for the synthesis of ATP.[1a]

Inspired by the natural construction of PSU, we report herein an artificial LHS entrapped in a cross-linked reverse vesicle (cRV). RVs are unstable bilayer compartments formed in organic solvents that coalesce quickly. Simple cross-linking yielded cRVs with tunable amounts of organic chromophores within their interior. Organic chromophores tend to aggregate uncontrollably in water because of their strong hydrophobicity. In our case, however, the compartmentation set the boundaries for the aggregation of hydrophobic chromophores with aggregation-induced emission (AIE).[13] The fluorescence quantum yield for our donor went from less than 0.002 in chloroform to up to 0.42 in water within the cRV. The final LHS displayed an EET efficiency of up to 95 % at a donor/acceptor ratio of 100:1. The quenching of donor was clearly detectable even at a donor/acceptor ratio of 10 000:1, making these systems one of the most efficient in the literature. Furthermore, our synthetic strategy enabled us to tune the emission color of the materials at will, simply by adjusting the donor/acceptor ratio, thanks to their complementary emission colors. White-light-emitting organic materials are extremely useful in illumination and sensing,[14] and our white-light-emitting cRVs had a quantum yield of 0.38, the highest reported to date in water, to the best of our knowledge.

The preparation of the cRVs is shown in Scheme 1. The structure of the amphiphile **1** is the key to the process. Its tetraethylene glycol (TEG) tails are soluble in chloroform and serve as the solvent-exposed portion of the bilayer membrane. Its carboxylate headgroup provides the main driving force for the formation of the RVs. Importantly, oligo(ethylene glycol) groups have good solubility in water, making it possible to transfer the RVs into water after cross-linking.

As shown in Figure 1 a, RVs were readily formed by hand-shaking the chloroform solution of **1** with a trace amount of water and had an average size of about 285 nm by dynamic

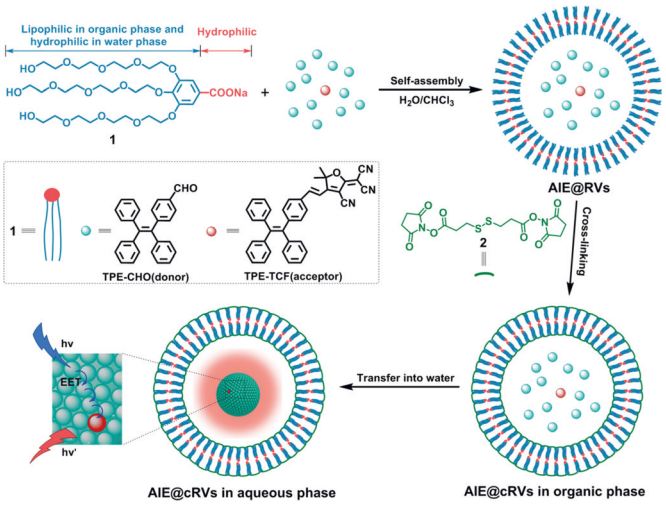

Scheme 1. Schematic representation of construction of the light-harvesting system AIE@cRVs.

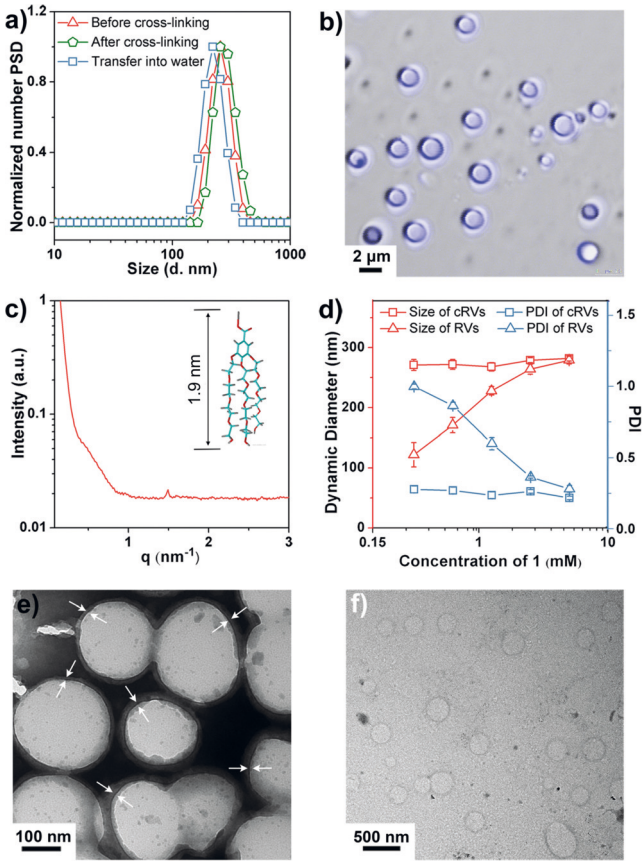

Figure 1. a) Distribution of dynamic diameters of RVs formed by **1** in chloroform, after cross-linking with **2** in chloroform, and after transfer of the cross-linked material into water. b) Fluorescence image of HPTS-loaded RVs in $CHCl_3$. c) SAXS spectrum of RVs in $CHCl_3$. The insert shows the molecular model of **1** generated by the ACD Labs software. d) Size and PDI (particle dispersion index) of RVs and cRVs as a function of the concentration of **1** in $CHCl_3$. The concentration-independent size and PDI verified the stability of covalently captured materials. e) TEM image of cRVs in $CHCl_3$. The arrows pointed to the wall of cRVs. f) TEM image of cRVs in water. [**1**] = 0.5 mM.

light scattering (DLS). The vesicular structure was supported by the entrapment of a hydrophilic dye, 8-hydroxy-1,3,6-pyrenetrisulfonic acid trisodium salt (HPTS).[15] As shown in Figure 1b, the HPTS-loaded RVs showed brighter emission near the periphery than the interior, consistent with a vesicular structure and dyes that adsorbed onto the membranes.[16] The vesicular structure was verified further by small-angle X-ray scattering (SAXS), which gave a wall thickness of 4.2 nm (Figure 1c), approximately twice the length of **1** (Figure 1c, insert), suggesting that the membranes were bilayers.

Like typical RVs, the resulting RVs of **1** were unstable and coalesced within 24 hours (see Figure S1a in the Supporting Information). However, when the RVs were treated with the *N*-hydroxysuccinimide ester **2** and *N*,*N*-dimethylaminopyridine (DMAP), stable cRVs were obtained readily (see the Supporting Information for details). The cross-linking was evident from the disappearance of the succinimide and hydroxy proton signals in the ^{1}H NMR spectra (see Figure S2).[17] After cross-linking, the vesicles remained similar in size (Figure 1a) but became far more stable in both long-term storage (see Figure S1b) and dilution tests (Figures 1d). Transmission electron microscopy (TEM) revealed a spherical structure for the cRVs (Figure 1e). The obvious contrast between the interior and the periphery once again supported membrane-enclosed vesicular assemblies.

The cRVs could be transferred easily from chloroform to water by removing the organic solvent through dialysis. Both the DLS and TEM measurements confirmed the maintenance of the vesicular structure after the transfer, except a slight decrease in size (Figures 1a,f). The size change is not surprising given the very different solvent environments (chloroform versus water). In a control experiment, when **1** was added directly to water, DLS showed no formation of nanoparticles. Since both the carboxylate and the TEG groups are hydrophilic, the molecule is not expected to self-assemble in any meaningful way without the cross-linking.

The dual solubility of cRVs in chloroform and water allowed us to load them with hydrophobic dyes directly in chloroform and use the membranes as the boundary to control the aggregation of the dyes in water. Organic dyes often display self-quenching and/or excimer formation upon aggregation. In this study, we used AIE-based hydrophobic dyes (TPE-CHO as the donor and TPE-TCF as the acceptor) to construct our LHSs.

Figure 2a shows that the donor-loaded cRVs (TPE-CHO@cRVs) had negligible fluorescence in chloroform but displayed strong cyan-colored emission once the cRVs were transferred into water. As a control, when Nile red was entrapped, the opposite was observed, with the cRVs exhibiting strong red emission in chloroform and little emission in water (Figure 2a) due to aggregation-caused quenching (ACQ). The quantum yield (QY) of TPE-CHO@cRVs was measured to be less than 0.002 in chloroform. Once transferred into water, the QY increased dramatically and, as designed, could be controlled readily through the loading of the dye in the cRVs, up to 0.42 with a loading of 11.3 mol% dye (see Supporting Information for the determination of the loading).

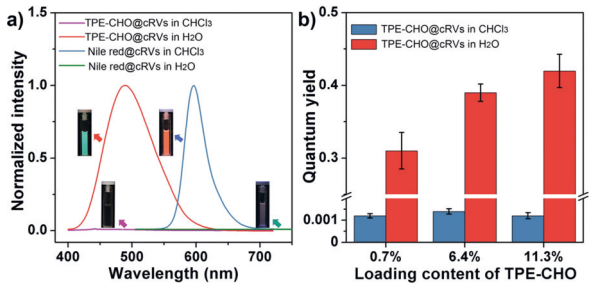

Figure 2. a) Fluorescence spectra of TPE-CHO@cRVs ($\lambda_{ex} = 372$ nm) and Nile red@cRVs ($\lambda_{ex} = 490$ nm) in $CHCl_3$ and in water. The inset shows the corresponding photographs under a hand-held UV lamp (365 nm). b) Comparison of QYs of TPE-CHO@cRVs in $CHCl_3$ and in water with different dye loadings.

As the acceptor, TPE-TCF absorption overlaps with the emission peak of the TPE-CHO donor (see Figure S3). Since both the donor and the acceptor are AIE-based and share a common backbone, their intimate mixing upon aggregation should be facile and facilitate EET. With the hydrophobic AIE dyes trapped in the interior of the cRVs, making a LHS is as simple as using a dye mixture in the preparation. To test the light-harvesting property, three batches of AIE@cRVs (**I**–**III**) with low (0.7 %), medium (6.4 %) and high (11.3 %) loadings of TPE-CHO were prepared. The donor/acceptor ratio was varied from 10 000:1 to 100:1.

As shown in Figures 3 a–c, excitation of these AIE@cRVs at 372 nm with increasing amounts of the acceptor, displayed decreasing donor emission at 480 nm and increasing acceptor emission at 570 nm, consistent with fluorescence resonance energy transfer (FRET) from the donor to the acceptor.[18] The energy-transfer efficiencies (Φ_{ET}) of the LHSs are shown in Figure 3 d and Table S1. At a 100:1 donor/acceptor ratio, a very impressive Φ_{ET} was obtained, that is, 83 %, 89 % and 95 %, for AIE@cRV **I**, **II**, and **III**, respectively. For AIE@cRV **III**, a significant Φ_{ET} (13 %) was observed even at a donor/acceptor ratio of 10 000:1, highlighting the efficiency of the system.

The energy transfer of AIE@cRV **III** was studied additionally by its fluorescence lifetime decay. The lifetime of the donor emission at 480 nm was 1.97 ns and decreased continuously, with increasing amounts of acceptor doped into the mixture, to 0.52 ns at a 100:1 donor/acceptor ratio (Figure 3 e, see Table S2). At this ratio, the time-resolved fluorescence spectra, excited at 371 nm, displayed a decrease of donor emission ($\lambda_{em} = 480$ nm) within 2 ns, accompanied by a sharp increase of the acceptor emission ($\lambda_{em} = 570$) (Figure 3 f).

The efficiency of a LHS is often measured by the average number of donor molecules quenched by a single acceptor and the antenna effect (AE) as described in the literature. The former could be obtained by the linear curve-fitting of the Stern–Volmer plot of the donor as a function of the donor/acceptor ratio (K_{SV}, Figure S6).[19] Our cRV-based LHSs were found to have outstanding K_{SV} values: 266 ± 17 for cRV **I**, 534 ± 23 for cRV **II**, and 689 ± 28 for cRV **III** (Figure 4 a). The increasing K_{SV} values with the higher loading of the dye in the cRV was reasonable given the positive correlation between the dye loading and donor's QY (Figure 2 b). The result

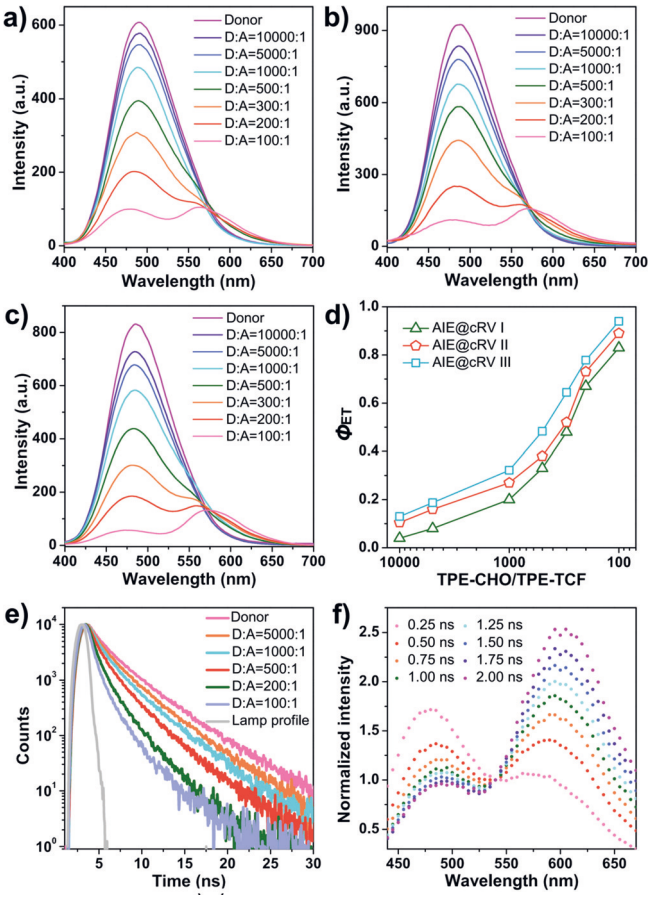

Figure 3. Fluorescence spectra of AIE@cRVs **I** (a), **II** (b), and **III** (c) in water at different donor/acceptor (D:A) ratios. d) Energy-transfer efficiencies (Φ_{ET}) of AIE@cRVs **I**–**III** as a function of D:A ratios. e) Fluorescence lifetime decay curves of AIE@cRV **III** at the donor's emission of 480 nm in water. f) Time-resolved fluorescence spectra of AIE@cRV **III** after excitation at 371 nm with the donor/acceptor ratio of 100:1. [T] = 0.5 mM.

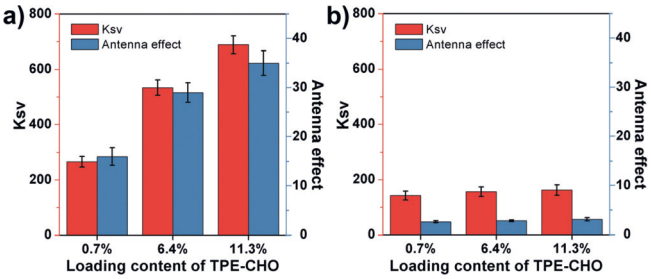

Figure 4. a) K_{SV} and AE of the AIE@cRVs **I**–**III**. b) K_{SV} and AE of the mixed aggregates of AIE@SLS.

suggests that a larger amount of the hydrophobic dye in the cRV aggregated more strongly and was helpful to the AIE. The AE displayed a similar trend: 16 ± 2 for cRV **I** (D:A = 500:1), to 27 ± 2 for cRV **II** (D:A = 1000:1), and 35 ± 3 for cRV **III** (D:A = 1000:1). It is worth noting that AIE@cRV **III**, with K_{SV} of 689 and AE of 35, outperforms the vast majority of artificial LHSs reported in the literature.[2–12,19]

White-light-emitting organic materials have gained much attention in recent years because of their potential in

illumination and sensing.[14] Thanks to the complementary emission colors of the TPE-CHO and TPE-TCF (i.e., cyan and orange), the emission of the dye-loaded cRVs can be tuned at will by simply changing the donor/acceptor ratio. As shown in Figure 5, the emission color of AIE@cRV **III** with

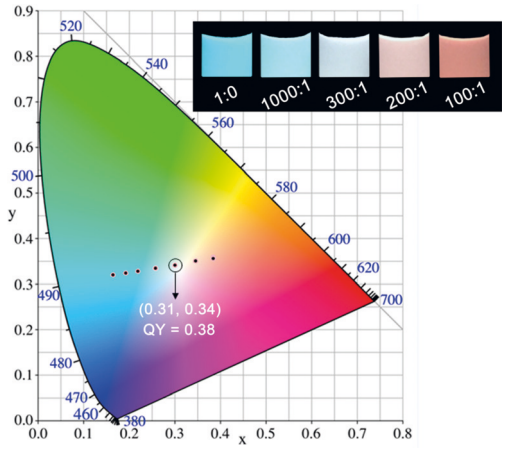

Figure 5. CIE 1931 chromaticity diagram showing the luminescence color coordinates of AIE@cRV **III** with different donor/acceptor ratios in water. The insert shows the corresponding fluorescence photographs under 365 nm UV light.

decreasing TPE-CHO/TPE-TCF ratios changed gradually from cyan to orange. Significantly, the sample with a 300:1 donor/acceptor ratio displayed a pure white-light emission with color coordinates of (0.31, 0.34), very close to the exact white point (0.33, 0.33). The quantum yield of the white light was 0.38 (see Table S3), the highest reported so far for white-light-emitting organic materials in water.

The strong performance of our LHSs in multiple aspects indicates that the cRV is an outstanding platform for light harvesting and luminescence. Two key factors were probably responsible for the results. First, the hydrophobically driven aggregation of the dyes put the fluorophores within very close distance. Our calculation affords a Förster radius of 3.3 nm for the donor–donor energy transfer and 4.6 nm for the donor–acceptor transfer (see Supporting Information for details). Since aggregation of hydrophobic molecules seeks to minimize the unfavorable exposure of hydrophobic surface, the dyes will be in intimate contact with one another. Normally, such aggregation is expected to cause quenching and/or excimer formation for hydrophobic fluorophores but actually enhances the QY of the AIE-based dyes, as shown in Figure 2b. All these factors collectively made it possible for the system to reach 95% Φ_{ET} for AIE@cRV **III** (Figure 3d). Second, the confined nanospace of the cRV set the boundary for the aggregation of donor and acceptor fluorophores and forced them to coaggregate at the intended ratio. Intermolecular interactions are known to increase, sometimes dramatically, when the molecules are confined in a nanospace.[20] Owing to enclosing in the cRVs, the donor and acceptor engage in an enhanced intermolecular interaction. Once transferred into water, they might prefer to coaggregate at the intended ratio, otherwise the phase separation of the two dyes would lower the number of the donor molecules around the acceptor, thus decreasing the overall efficiency of system (see Figure S4). As a control, we prepared coaggregates of TPE-CHO and TPE-TCF by reprecipitation from their tetrahydrofuran solution into an aqueous solution of sodium laurylsulfonate (SLS). The materials obtained (AIE@SLS) represent traditional organic nanoparticles prepared without the membrane boundary of cRVs and thus any potential nanoconfinement. As shown in Figures 4b, Figures S5–S7, and Table S4, the energy transfer was significantly less efficient and the highest K_{SV} and AE values achieved were, respectively 162 and 3.3, in sharp contrast to the 689 and 35 obtained for AIE@cRV **III** (Figure 4a).

Once again, the natural design with dyes aggregating in a confined nanospace proves superior to those relying on special organic frameworks to arrange the dyes. When we created similar biomimetic LHSs as a primitive chloroplast using cRVs, the membrane-enclosed structure clearly facilitated the self-assembly and the energy transfer of the entrapped donor/acceptor dyes. This platform gives us tremendous flexibility with regard to the type, amount, and ratio of dyes loaded into the vesicles. Importantly, aggregation of the dyes occurs spontaneously through hydrophobic interactions and the intimate contact of the dyes was optimal for AIE-based fluorophores and the EET of the system. In addition to the potential of the cRVs in light harvesting and emission, the tunable multicolored emission and water-compatibility of our platform holds great promise in bioimaging and sensing. Applications of these materials are currently being investigated and will be reported in due course.

Acknowledgements

This work was supported by the National Natural Science Foundation of China (51673130), NSF (CHE-1708526), the National 111 Project of Introducing Talents of Discipline to Universities (No. B16033), and the Applied Basic Research Project of Sichuan Province (No. 15JC0440). We are grateful to Prof. Qing-Zheng Yang (Beijing Normal University) for valuable discussions and manuscript preparation. We also thank Prof. Peng Wu (Sichuan University) for the time-resolved fluorescence measurement, and the Center of Testing and Analysis, Sichuan University, for NMR and TEM measurements.

Conflict of interest

The authors declare no conflict of interest.

Keywords: aggregation · energy transfer · light harvesting · nanostructures · vesicles

[1] a) N. Nelson, A. Ben-Shem, *Nat. Rev. Mol. Cell Biol.* **2004**, *5*, 971 – 982; b) T. Mirkovic, E. E. Ostroumov, J. M. Anna, R. van Grondelle, Govindjee, G. D. Scholes, *Chem. Rev.* **2017**, *117*, 249 – 293.

[2] a) Y. Wang, H. Suzuki, J. Xie, O. Tomita, D. J. Martin, M. Higashi, D. Kong, R. Abe, J. Tang, *Chem. Rev.* **2018**, *118*, 5201 – 5241; b) H.-Q. Peng, L.-Y. Niu, Y.-Z. Chen, L.-Z. Wu, C.-H. Tung, Q.-Z. Yang, *Chem. Rev.* **2015**, *115*, 7502 – 7542; c) G. J. Hedley, A. Ruseckas, I. D. Samuel, *Chem. Rev.* **2017**, *117*, 796 – 837.

[3] a) Y. H. Jeong, M. Son, H. Yoon, P. Kim, D. H. Lee, D. Kim, W. D. Jang, *Angew. Chem. Int. Ed.* **2014**, *53*, 6925 – 6928; *Angew. Chem.* **2014**, *126*, 7045 – 7048; b) D. Yim, J. Sung, S. Kim, J. Oh, H. Yoon, Y. M. Sung, D. Kim, W. D. Jang, *J. Am. Chem. Soc.* **2017**, *139*, 993 – 1002.

[4] a) K. V. Rao, K. K. Datta, M. Eswaramoorthy, S. J. George, *Angew. Chem. Int. Ed.* **2011**, *50*, 1179 – 1184; *Angew. Chem.* **2011**, *123*, 1211 – 1216; b) A. Ajayaghosh, V. K. Praveen, C. Vijayakumar, S. J. George, *Angew. Chem. Int. Ed.* **2007**, *46*, 6260 – 6265; *Angew. Chem.* **2007**, *119*, 6376 – 6381; c) T. Gorai, U. Maitra, *Angew. Chem. Int. Ed.* **2017**, *56*, 10730 – 10734; *Angew. Chem.* **2017**, *129*, 10870 – 10874.

[5] a) G. Chadha, Q.-Z. Yang, Y. Zhao, *Chem. Commun.* **2015**, *51*, 12939 – 12942; b) H.-Q. Peng, Y.-Z. Chen, Y. Zhao, Q.-Z. Yang, L.-Z. Wu, C.-H. Tung, L.-P. Zhang, Q.-X. Tong, *Angew. Chem. Int. Ed.* **2012**, *51*, 2088 – 2092; *Angew. Chem.* **2012**, *124*, 2130 – 2134; c) Y. Liu, J. Jin, H. Deng, K. Li, Y. Zheng, C. Yu, Y. Zhou, *Angew. Chem. Int. Ed.* **2016**, *55*, 7952 – 7957; *Angew. Chem.* **2016**, *128*, 8084 – 8089.

[6] a) C. F. Calver, K. S. Schanze, G. Cosa, *ACS Nano* **2016**, *10*, 10598 – 10605; b) X. Zhang, S. Rehm, M. M. Safont-Sempere, F. Wurthner, *Nat. Chem.* **2009**, *1*, 623 – 629.

[7] a) Z. Xu, S. Peng, Y.-Y. Wang, J.-K. Zhang, A. I. Lazar, D.-S. Guo, *Adv. Mater.* **2016**, *28*, 7666 – 7671; b) J.-J. Li, Y. Chen, J. Yu, N. Cheng, Y. Liu, *Adv. Mater.* **2017**, *29*, 1701905; c) S. Guo, Y. Song, Y. He, X. Y. Hu, L. Wang, *Angew. Chem. Int. Ed.* **2018**, *57*, 3163 – 3167; *Angew. Chem.* **2018**, *130*, 3217 – 3221; d) C.-L. Sun, H.-Q. Peng, L.-Y. Niu, Y.-Z. Chen, L.-Z. Wu, C.-H. Tung, Q.-Z. Yang, *Chem. Commun.* **2018**, *54*, 1117 – 1120.

[8] a) Y. Sun, Y. Lei, L. Liao, W. Hu, *Angew. Chem. Int. Ed.* **2017**, *56*, 10352 – 10356; *Angew. Chem.* **2017**, *129*, 10488 – 10492; b) P.-Z. Chen, Y.-X. Weng, L.-Y. Niu, Y.-Z. Chen, L.-Z. Wu, C.-H. Tung, Q.-Z. Yang, *Angew. Chem. Int. Ed.* **2016**, *55*, 2759 – 2763; *Angew. Chem.* **2016**, *128*, 2809 – 2813; c) M. Sun, Y. Liu, Y. Yan, R. Li, Q. Shi, Y. Zhao, Y. Zhong, J. Yao, *J. Am. Chem. Soc.* **2018**, *140*, 4269 – 4278; d) M. Sun, Y. Zhong, J. Yao, *Angew. Chem. Int. Ed.* **2018**, *57*, 7820 – 7825; *Angew. Chem.* **2018**, *130*, 7946 – 7951.

[9] a) D. E. Williams, J. A. Rietman, J. M. Maier, R. Tan, A. B. Greytak, M. D. Smith, J. A. Krause, N. B. Shustova, *J. Am. Chem. Soc.* **2014**, *136*, 11886 – 11889; b) H. J. Son, S. Jin, S. Patwardhan, S. J. Wezenberg, N. C. Jeong, M. So, C. E. Wilmer, A. A. Sarjeant, G. C. Schatz, R. Q. Snurr, O. K. Farha, G. P. Wiederrecht, J. T. Hupp, *J. Am. Chem. Soc.* **2013**, *135*, 862 – 869; c) C. A. Kent, D. Liu, L. Ma, J. M. Papanikolas, T. J. Meyer, W. Lin, *J. Am. Chem. Soc.* **2011**, *133*, 12940 – 12943.

[10] a) C. B. Winiger, S. Li, G. R. Kumar, S. M. Langenegger, R. Haner, *Angew. Chem. Int. Ed.* **2014**, *53*, 13609 – 13613; *Angew. Chem.* **2014**, *126*, 13828 – 13832; b) Y. Shi, X. Cao, D. Hu, H. Gao, *Angew. Chem. Int. Ed.* **2018**, *57*, 516 – 520; *Angew. Chem.* **2018**, *130*, 525 – 529.

[11] a) P. Ensslen, H. A. Wagenknecht, *Acc. Chem. Res.* **2015**, *48*, 2724 – 2733; b) J. G. Woller, J. K. Hannestad, B. Albinsson, *J. Am. Chem. Soc.* **2013**, *135*, 2759 – 2768; c) P. K. Dutta, R. Varghese, J. Nangreave, S. Lin, H. Yan, Y. Liu, *J. Am. Chem. Soc.* **2011**, *133*, 11985 – 11993; d) L. Zhao, H. Zou, H. Zhang, H. Sun, T. Wang, T. Pan, X. Li, Y. Bai, S. Qiao, Q. Luo, J. Xu, C. Hou, J. Liu, *ACS Nano* **2017**, *11*, 938 – 945.

[12] a) S. Kundu, A. Patra, *Chem. Rev.* **2017**, *117*, 712 – 757; b) A. Reisch, P. Didier, L. Richert, S. Oncul, Y. Arntz, Y. Mely, A. S. Klymchenko, *Nat. Commun.* **2014**, *5*, 4089; c) K. Trofymchuk, A. Reisch, P. Didier, F. Fras, P. Gilliot, Y. Mely, A. S. Klymchenko, *Nat. Photonics* **2017**, *11*, 657 – 663.

[13] a) J. Luo, Z. Xie, J. W. Y. Lam, L. Cheng, H. Chen, C. Qiu, H. S. Kwok, X. Zhan, Y. Liu, D. Zhu, B. Z. Tang, *Chem. Commun.* **2001**, 1740 – 1741; b) J. Mei, N. L. Leung, R. T. Kwok, J. W. Lam, B. Z. Tang, *Chem. Rev.* **2015**, *115*, 11718 – 11940.

[14] a) H.-Q. Peng, C.-L. Sun, L.-Y. Niu, Y.-Z. Chen, L.-Z. Wu, C.-H. Tung, Q.-Z. Yang, *Adv. Funct. Mater.* **2016**, *26*, 5483 – 5489; b) M. Zhang, S. Yin, J. Zhang, Z. Zhou, M. L. Saha, C. Lu, P. J. Stang, *Proc. Natl. Acad. Sci. USA* **2017**, *114*, 3044 – 3049.

[15] a) K. D. Zhang, T. Y. Zhou, X. Zhao, X. K. Jiang, Z. T. Li, *Langmuir* **2012**, *28*, 14839 – 14844; b) H. Li, X. Xin, T. Kalwarczyk, E. Kalwarczyk, P. Niton, R. Holyst, J. Hao, *Langmuir* **2010**, *26*, 15210 – 15218; c) H. Kunieda, K. Nakamura, M. R. Infante, C. Solans, *Adv. Mater.* **1992**, *4*, 291 – 293.

[16] Note that the size of the nanoparticles observed in the fluorescence image is much larger than that observed by DLS assay. This difference is ascribed to the diffraction limit of fluorescence microscope, which makes the original RVs hard to observe, whereas the fused large nanoparticles can be readily observed, although they are minority. Related examples, see [7c,15a].

[17] a) Y. Chen, J. Huang, S. Zhang, Z. Gu, *Chem. Mater.* **2017**, *29*, 3083 – 3091; b) Y. Liu, Y. Chen, Y. Yao, K. Luo, S. Zhang, Z. Gu, *Langmuir* **2017**, *33*, 5275 – 5282; c) C. Liao, Y. Chen, Y. Yao, S. Zhang, Z. Gu, X. Yu, *Chem. Mater.* **2016**, *28*, 7757 – 7764.

[18] C.-B. Huang, L. Xu, J.-L. Zhu, Y.-X. Wang, B. Sun, X. Li, H.-B. Yang, *J. Am. Chem. Soc.* **2017**, *139*, 9459 – 9642.

[19] a) C. F. Wu, Y. L. Zheng, C. Szymanski, J. McNeill, *J. Phys. Chem. C* **2008**, *112*, 1772 – 1781; b) E. J. Harbron, C. M. Davis, J. K. Campbell, R. M. Allred, M. T. Kovary, N. J. Economou, *J. Phys. Chem. C* **2009**, *113*, 13707 – 13714; c) S. Bhattacharyya, B. Paramanik, A. Patra, *J. Phys. Chem. C* **2011**, *115*, 20832 – 20839.

[20] a) J. Baugh, A. Kleinhammes, D. X. Han, Q. Wang, Y. Wu, *Science* **2001**, *294*, 1505 – 1507; b) S. Krishnamoorthy, M. Himmelhaus, *Adv. Mater.* **2008**, *20*, 2782 – 2788; c) Y. Chen, S. Wang, J. Ye, D. Li, Z. Liu, X. Wu, *Nanoscale* **2014**, *6*, 9563 – 9567; d) L.-J. Chen, S. Chen, Y. Qin, L. Xu, G.-Q. Yin, J.-L. Zhu, F.-F. Zhu, W. Zheng, X. Li, H.-B. Yang, *J. Am. Chem. Soc.* **2018**, *140*, 5049 – 5052.